CHAPTER 1

INTRODUCTION AND LITERATURE SURVEY

1.1 Introduction

Magnetic materials, especially permanent magnets (PMs), play a vital role in different application areas because of their characteristic property of providing high power in a small volume. They provide magnetic flux without any energy input. Due to the industrial revolution, their practical involvement are now extended to support various application areas such as electric vehicles, motor drives, generators, automobiles, recording media, microwave devices, medical apparatuses, and several others, as presented in Fig. 1.1. The huge global demand for PMs and their market capitalizations are rapidly increasing and is estimated to $34.7 billion market value by 2026, which is projected with CAGR of 8.7% (Permanent Magnet Market, 2020). In the PM category, four types of magnets are highly attractive: NdFeB, SmCo, Alnico, and ferrite magnets. A comparison between these magnets in terms of magnetic properties and price statics are listed in Table 1.1. Rare-earth (RE) contained magnets (NdFeB and SmCo) are the most preferred PMs due to their high energy density. However, China has a monopoly in RE elements due to geographical resources. It results in price instability and supply shortage of RE elements due to the imposition of different export policies as well as increment in the price of RE elements by many folds. Also, NdFeB magnets are more environmentally harmful than the other materials utilized in electrical motor drives. Even if the mass of NdFeB is only 5% of the electric motor drives, it may be responsible for about 25% of material-related greenhouse gas emissions (Widmer et al., 2015).

Due to the recent boom in cleaner and environment-friendly engineering, today's technological requirements are pushing the demand for permanent magnets to move on

towards the development of rare-earth free permanent magnets. It leads to the research of new materials and improvements in the functional properties of the existing ones. Among the four leading permanent magnets, NdFeB and SmCo are not acceptable in the ecological and green-future-related objectives due to the high cost, unstable market, global warming, and energy problem associated with the RE elements. Alnico magnets have high remanent flux density but very low coercivity, resulting in a high demagnetization risk (Widmer et al., 2015). It indicates that perhaps a ferrite magnet is an absolute choice. Many researchers have reported their testing for the ferrite PM to replace the NdFeB magnets in energy conversion applications (Jeong et al., 2021; Kakihara et al., 2013; Kim et al., 2014; Luk et al., 2020; Sanada et al., 2011; Widmer et al., 2015), which suggests a strong possibility that ferrite PM can be a decent competitor to NdFeB. In ceramic ferrite magnets, nearly all hexagonal ferrite magnets are made using strontium due to the environmental and safety concerns associated with lead and barium. Strontium hexaferrite magnets are the world's largest produced magnet, contributing >80% to the total volume of globally manufactured permanent magnets each year (Cui et al., 2022).

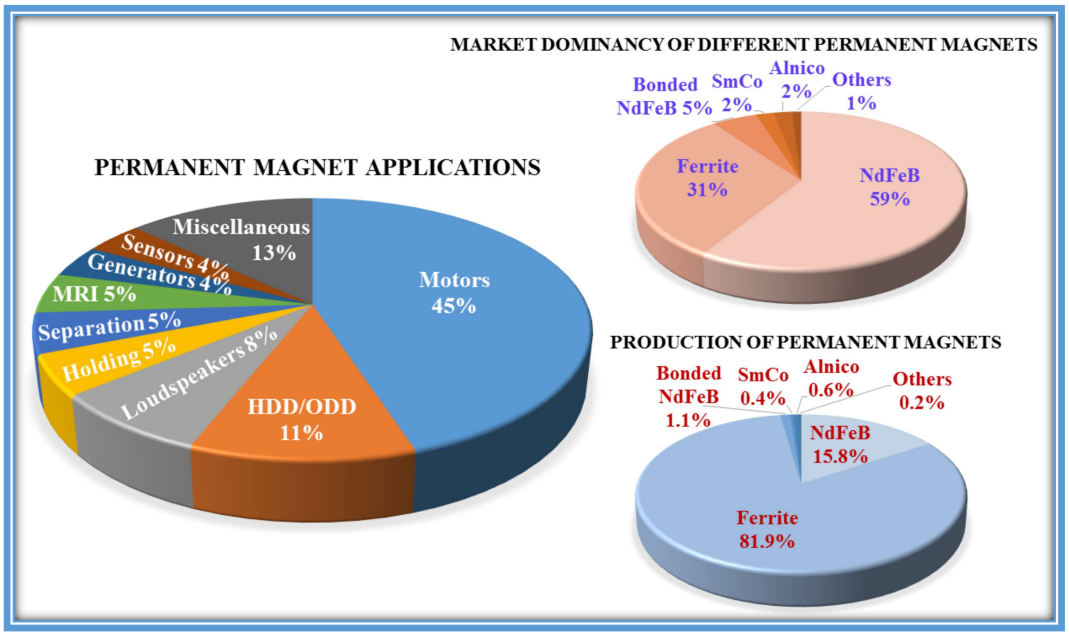

Figure 1.1 *Applications of PMs by market share, market dominancy and production of different PMs in 2019 [data collected from* (John Ormerod, 2019)*].*

Table 1.1 *Comparison of magnetic properties and price of different commercial permanent magnets [data collected from* (Coey, 2010; Cui et al., 2018)*].*

Magnet	$(BH)_{max}$ (MGOe)	T_C (^oC)	$T_{f_{max}}$ (^oC)	iH_c (kOe)	M_s (T)	M_r (T)	ρ (μΩ-cm)	Estimated price ($/kg)
$Nd_2Fe_{14}B$	43.98	315	160	12.57	1.54	1.28	150	$120
Sm_2Co_{17}	27.65	917	350	13.82	1.15	1.08	90	$210
$SmCo_5$	18.85	747	250	21.36	0.95	0.88	60	$210
Alnico 5	5.40	860	550	0.68	1.40	1.25	50	$80
$SrFe_{12}O_{19}$	4.27	473	250	3.46	0.47	0.42	10^{10}	$4

In the present thesis, rare-earth free permanent magnets is tried to develop with improved magnetic properties. Considering the featured properties of strontium hexaferrite such as magnetic properties, ease of processing, price stability, and performance balance, it is selected here as the base material for the desired objective.

1.2 Overview of Magnetic Parameters

Magnetic properties are the most vital characteristics of permanent magnets, making them unique from electromagnets. In electromagnets, continuous electric current is required to operate and generate a magnetic field. However, PM can produce a magnetic field without any energy input. There are a few key magnetic parameters for the development of a high-performance rare-earth free permanent magnet. Towards the goal of improving the magnetic characteristics of SrM magnets, these parameters need to be discussed first.

Curie temperature (T_c) is defined as the transition temperature where ferromagnetic/ferrimagnetic materials undergo a paramagnetic state transition. In this transition, spins order changes from collinear to non-collinear. It defines the temperature limit above which extensive thermal energy becomes enough to depredate the magnetic ordering. The temperature reliance of materials arises from the magnetic sub-lattices having

different temperature-dependent characteristics. It comes due to the rapid increase in the net magnetization than the anisotropy constant with a temperature decrease. T_c falloffs due to the spin-canting structure that causes the deviation in collinear arrangements of magnetic moment and can be enhanced by improving the exchange interaction between Fe ions. For ferrite magnets, -40°C is the temperature limit for practical applications. At this temperature, coercivity goes down to its minimum, making devices inoperable at higher altitudes during winter (Kramer et al., 2012). During the operation process of electrical machines, the magnet may be subject to an excess temperature of ~100°C. When the temperature reaches the T_c point, both M_s and H_c naturally falloffs. Some losses are not recoverable on coming back to the ambient temperature; those are known as irreversible losses and are triggered by thermal cycling. It limits the effective use of magnets to a maximum functioning temperature ($T_{f_{max}}$) and are listed in Table 1.1.

Energy density [$(BH)_{max}$] is known as the key figure of merit for the performance assessment of permanent magnets. It is estimated by the highest rectangular area that can be best fitted in the demagnetization curve, i.e., II-quadrant of the *B-H* loop. A straight demagnetization curve is desirable to support a broad range of speeds with stable power operation. Magnets are operable at all points in this straight *B-H* curve by sustaining their hard magnet properties. High $(BH)_{max}$ is desirable for product miniaturization and reduced electrical power consumption as it can support generating a larger flux density in a smaller volume. Low $(BH)_{max}$ value can be compensated by the bulk volume of magnetic materials, but it will increase the size of devices. A high value of $(BH)_{max}$ is associated with the other magnetic parameters as well. A large M_r and large H_c values are needed for the maximum optimized $(BH)_{max}$ value. Consequently, the high coercive field and high remanence-induction result in strong resistance to demagnetization and large energy product.

Magnetocrystalline anisotropy (K) is the magnitude of energy needed to rotate the magnetic moment away from the easy magnetization axis. It is an intrinsic magnetic property of a material, which is influenced by the structural symmetry of the compound. In M-type strontium hexaferrite structure, lattice sites *2b* (↑) and $4f_2$ (↓) significantly contribute to the K parameter (Roohani et al., 2017). The role of trigonal bipyramidal site (*2b*) is very decisive for high K value in SrM because Fe ions of this site are not positioned directly in the center but are located between the two adjacent pseudo-tetrahedron. The improvement in magnetocrystalline anisotropy is interconnected with the influence of orbital moment or change in chemical & crystal structures, which causes a local increase in magnetic anisotropy. Additionally, the hexagonal structure creates the anisotropy to consist along the *c*-axis. Alteration of anisotropy constant from positive to negative designates the conversion of *c*-axis magnetocrystalline anisotropy into a favored magnetization plane (Fang et al., 2001). The purpose of selecting SrM is due to their large uniaxial magnetocrystalline anisotropy field (>1.5 T), producing substantial coercive fields. It is the physical origin of coercivity, which sets the maximum limit of H_c that can be realized in a material.

Coercivity (H_c) is the measure of ability of any material to withstand externally applied field without getting demagnetized. The H_c value describes the remanent state stability and classifies magnets into hard (high H_c) and soft (low H_c) magnetic material. A high value of H_c is desirable for permanent magnets. H_c is an extrinsic parameter whose physical origin is the magnetocrystalline anisotropy field. It increases with magnetocrystalline anisotropy. Also, H_c is more likely dependent on the shape and size of the particles and varies inversely with grain size. The H_c dependency on the grain size (D) is displayed in Fig 1.2. The H_c value is almost zero for single-domain particle size less than the critical diameter of super-paramagnetism (D_{spm}). A single magnetic-domain structure

may improve the H_c value because only one stable magnetic domain exists if the grain size is smaller than the critical single-domain grain size (D_s). Further grain growth beyond the D_s threshold may decrease the H_c. The magnetization reversal process is coherent rotation in a single magnetic domain due to the absence of a domain wall. According to the Stoner-Wohlfarth theory, a maximum value of H_c can be achieved by the magnetization reversal of a single magnetic domain particle resulting from the coherent rotation of the magnetic vector from one easy axis to another. In addition to the coherent rotation, nucleation and domain wall pinning can also strengthen the H_c (Mohapatra & Liu, 2018).

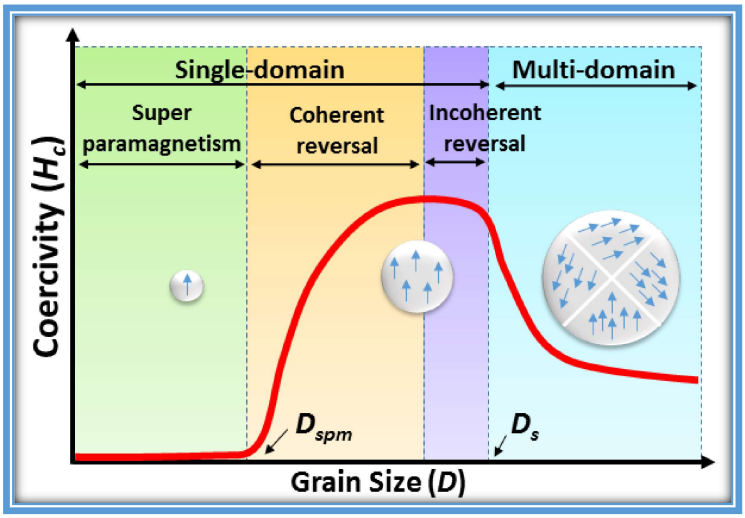

Figure 1.2 *Dependency of coercivity on grain size D; D_{spm} is the critical grain size that results in superparamagnetism, and D_s is the critical grain size for the single domain* (de Julián Fernández et al., 2021).

Saturation magnetization (M_s) is a measure of maximum magnetic moment per unit volume. It is an intrinsic property of materials, which highly depends on the atomic origin of magnetism and involves quantum phenomena like exchange interaction, interatomic hopping, crystal field interaction, and spin-orbit coupling (Skomski & Sellmyer, 2008). The M_s value is required to be large for application purposes. A large value of M_s allows miniaturization, one of the essential characteristic requirements in today's modern application areas. The net magnetic moment plays a vital role in M_s of ferromagnetic

material and can be estimated by Eq. (1.1) in $SrFe_{12}O_{19}$ (= $20\mu_B$ per formula unit and $40\mu_B$ per unit cell). It is influenced by the site occupancy, valence state, density, ionic radius, etc., which are responsible for affecting the superexchange interaction between Fe_A^{3+}-O^{2-}-Fe_B^{2+}. The weakening of Fe ions interaction results in a decrease of M_s. The impurity phases, such as α-Fe_2O_3, may also decrease the M_s value. If substitutions of less magnetic ions than iron ions are forced to replace Fe ions from *2a* (↑), *2b* (↑), or *12k* (↑) lattice sites, the net magnetic moment will decrease and hence M_s will reduce, while if Fe ions are replaced from $4f_1$ (↓) or $4f_2$ (↓) lattice sites, it will increase M_s. Density improvement may also lead to high M_s value and the high strength of the magnet (Jean et al., 2010). The addition of various sintering aids and optimized processing temperature may result in the densification of material and hence increase in M_s.

$$1\overrightarrow{Fe}_{2b} + 1\overrightarrow{Fe}_{2a} + 6\overrightarrow{Fe}_{12k} - 2\overleftarrow{Fe}_{4f_2} - 2\overleftarrow{Fe}_{4f_1} = 20\mu_B(\uparrow) \qquad (1.1)$$

Remanent magnetization (M_r) is the residual magnetism left behind in the sample after removing the externally applied field. It is an extrinsic magnetic property of materials that depends on the history of samples, including everything that affects the size and texture of grains (Fersi et al., 2014). Higher M_r is desirable to increase the $(BH)_{max}$ of the material. A high M_s is desirable, which may indirectly benefit in obtaining a considerable M_r value. Though the M_s can be improved by substituting elements, this approach could reduce the exchange interaction among Fe ions. Large M_r can be obtained with easy axis alignment and improving magnetic intergranular interaction. Considerable enhancement in M_r is tough to attain because the magnetic coupling is generated on the antiferromagnetic exchange among the magnetic sublattices across O_2 atoms.

Being an oxidized material, strontium hexaferrite delivers decent oxidation and corrosion resistance, offering greater life expectancy. SrM is also famous for being resistant to different environmental stress. These magnets convey significant thermal

demagnetization resistance with increasing temperature, which is vital from the application perspective. With the discovery of ferrite magnets, the field of PMs went through a paradigm shift as the 'shape barrier' was broken by these magnets (Cui et al., 2022). Therefore, these magnets have good machining properties that allow them to cut into desired shapes and sizes. Additionally, decent magnetic properties and magnetic tunability of the strontium hexaferrite magnet are drawing attention to the feasibility of this magnet to make it a better rare-earth free PM.

1.3 Strontium Hexaferrite Magnet

The Philips laboratories first discovered strontium hexaferrite ($SrFe_{12}O_{19}$) in 1950. Since then, various studies have significantly upgraded the functional properties of these magnets with the optimization of synthesis parameters and substitution of different elements. The unique combination of characteristic properties, steady low price, and well-established manufacturing process is the key to its recognition and market significance. It comes under a magnetoplumbite (M-type) hexagonal structure with the configuration of ($A^{2+}O_{16}B_2^{3+}O_3$), as presented in Fig 1.3. The crystal structure of SrM can be described as a close-packed configuration of anions (O^{2-}) where voids are filled with cations (Sr^{2+} and Fe^{3+}), allowing the sequence of spinel S block ($Fe_6O_8^{2+}$) and hexagonal R block ($SrFe_6O_{11}^{2-}$), specified in Fig 1.4. The unit cell of SrM consists of two molecular units (64 ions), among which Sr^{2+} ions are located at the 2*d* lattice site. Fe^{3+} ions are distributed in five distinct and inequivalent lattice sites, as listed in Table 1.2. Superexchange interactions couple these lattice sites of Fe ion through O^{2-} ions, which are distributed in 4*e*, 4*f*, 6*h*, 12k_1, and 12k_2 lattice sites and are accountable for the magnetic properties in SrM magnets. It is a ferromagnetic material and has characteristic properties of high Curie temperature (732 K) (Pullar, 2012), high saturation magnetization (72 emu/g; theoretically) (Lee et al., 2020), high coercivity (7.5 kOe; theoretically) (Torkian et al., 2016), large magnetocrystalline

anisotropy (~350 kJ/m^3) (Eikeland et al., 2018), high resistivity (10^{10} μΩ-cm) (Coey, 2010), high corrosion & oxidation resistance, good chemical & thermal stability. SrM has a $(BH)_{max}$ limit of 2.6 to 4.8 MGOe, depending on the grades. The high value of $(BH)_{max}$ is a major challenge in this magnet, which is required to achieve towards the objective of high performing rare-earth free permanent magnet.

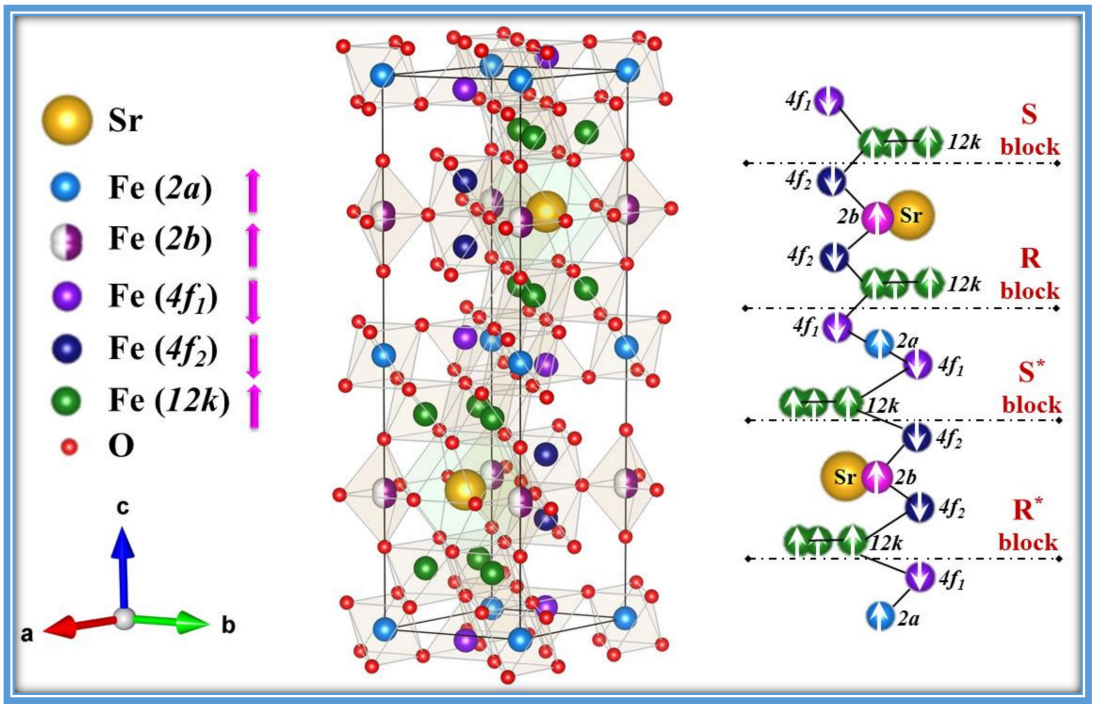

Figure 1.3 *M-type hexagonal structure of strontium hexaferrite.*

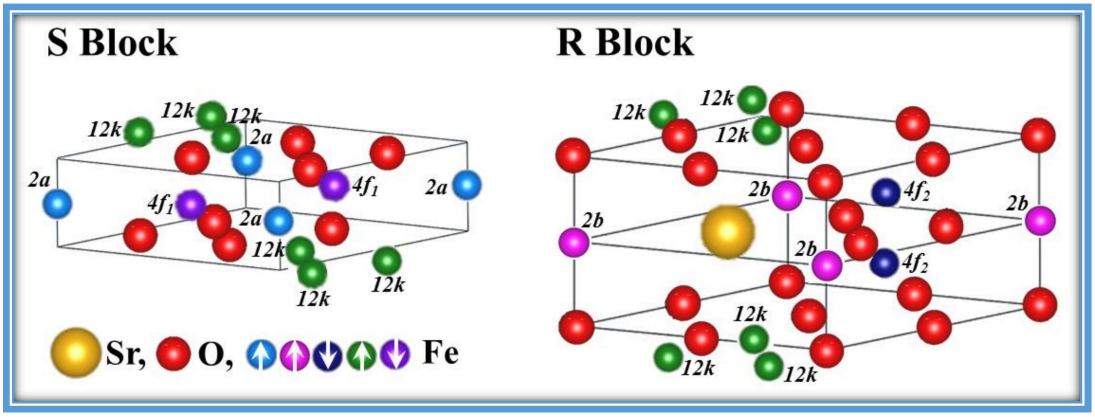

Figure 1.4 *Structure of S (spinel layer of $Fe_6O_8^{2+}$) & R (hexagonal layer of $SrFe_6O_{11}^{2-}$) blocks.*

Table 1.2 *Different lattice sites for Fe ion distribution in M-type hexaferrite.*

Block	Sites	Coordination	Symmetry	Spin direction	Ions per unit-cell
S	$4f_1$	tetrahedral	$3m$	(↓)	4
S	$2a$	octahedral	$\bar{3}m$	(↑)	2
R-S	$12k$	octahedral	M	(↑)	12
R	$4f_2$	octahedral	$3m$	(↓)	4
R	$2b$	bi-pyramidal	$\bar{6}m$	(↑)	2

1.4 Criteria for Development of Permanent Magnet

A high-performance permanent magnet requires large $(BH)_{max}$. A high value of $(BH)_{max}$ is associated with the increase in remanence (M_r) and coercivity (H_c). If $(BH)_{max}$ of SrM magnets can be improved, even slightly, it would open up a door to an extensive range of applicability due to the feasible magnetic tunability characteristic of SrM. For the development of rare-earth free PM, certain criteria need to be fulfilled, which are associated with the magnetic characteristics and large energy density in the magnets, as follows:

a) High H_c (resistance to demagnetization)

A large H_c value allows a sufficient safety margin to the sudden risk of demagnetization, which is beneficial from the application perspective. High coercivity can be attained by either the high magnetocrystalline anisotropy, small particle/grain size, or shape anisotropy.

b) High M_s (moment alignment)

High M_s is essential for high energy density. Theoretically, $(BH)_{max}$ is limited to $M_s^2/4$ and it is only achieved ≤ 80% of this maximum limit even after years of effort (Cui et al., 2022). High M_s and a high degree of grains alignment along the easy magnetic axis are required to improve M_r (magnetic strength).

c) High T_c (magnetic ordering)

During the application, the magnetic properties must be retained in the magnet for proper functionality, and T_c specifies how far above room temperature it could function effectively. High $T_c \geq 227^oC$ needs to be fulfilled as the rule of thumb so that magnet can meet its desired function during relevant application (Cui et al., 2022). The most-essential magnetic properties, i.e., both M_s and H_c begin to drop sharply above ~80% of T_c. The decrease in H_c is often quicker than M_s with the temperature, which points out the requirement of high T_c in permanent magnets.

SrM magnets possess tunable magnetic properties by different optimization in synthesis parameters as well as substitution of different elements. The magnetic properties of hexaferrite are highly influenced by the cation distribution among the crystallographic lattice sites. Synthesis methods significantly affect the cationic distribution, exchange-interaction strength, grain morphology, and particle size distribution. It implies that the synthesis method should be selected according to the desired properties based on targeted applications. Also, the substitution of different elements at Fe or Sr lattice sites influences the anisotropic crystal structure of SrM and hence the magnetic properties. The current progress in the magnetic properties of SrM with different synthesis techniques and the substitution of various non-rare-earth elements is briefly tried to cover in the following sections for high M_s and high H_c values in strontium hexaferrite magnets.

1.5 Literature Survey on Synthesis Techniques for SrM

The controlled synthesis process plays a crucial role in preparing a high-quality permanent magnet. All permanent magnets are preferentially manufactured by the powder metallurgy process, though there are some differences at a few stages for preparing different PMs. Strontium hexaferrite magnets can be prepared by many synthesis processes,

and the effect of these processes on the magnetic properties of SrM is briefly discussed here.

1.5.1 Solid-state Reaction Process

At the industrial scale, SrM magnets are prepared by the solid-state reaction due to mass production and simplified processing. It is also known as the traditional ceramic route or powder metallurgy process. It is a top-down approach in which starting materials are taken into a stoichiometric ratio and mixed by the milling process. The mechanochemical process results in powder size reduction and increases surface areas due to the repetitive compressive effect of balls. A high calcination temperature between 1000-1350^{o}C is required for the SrM phase formation. In this process, powder outcome depends on various parameters like reactants' reactivity towards each other, milling media, media to powder weight ratio, rotation speed and time, etc.

(Nourbakhsh et al., 2011) have optimized this process by SrO to Fe_2O_3 ratio at 1:6, T_{cal} at 1210^{o}C, and T_{sin} at 1220^{o}C to obtain better magnetic properties in SrM. (Kang et al., 2015) have found an enhanced value of H_c at Fe/Sr = 12, whereas improvement in M_s is found at Fe/Sr = 11 with T_{cal} at 1000^{o}C/4 h and T_{sin} at 1200^{o}C/4 h. (Stingaciu et al., 2015) have reported that about 12 hrs of ball-milling can give a better $(BH)_{max}$ value. Extended ball-milling time ($\geq$ 20 hrs) may cause an increment in M_s but a reduction in H_c. In SrM, a transition from multi to single-domain structures occurs below 500 nm, so the H_c value can be expected to increase with the milling time. M_s is more sensitive to the milling parameters (Jin et al., 1998) and T_{ann} (Sánchez-De Jesús et al., 2014) than H_c. The M_s of 72.2 emu/g and H_c of 5.01 kOe can be obtained in SrM with a ball/powder ratio of 7.5:1, milling speed at 250 rpm, and annealing at 1100^{o}C as reported by (Jin et al., 1998). They have conveyed that T_{ann} = 1100^{o}C is a suitable temperature for obtaining better magnetic properties of SrM through this process due to proper crystallization. (Sharma et al., 2006) have optimized the

process parameters such as SrO/Fe_2O_3 at 5, milling time for 1 hr, T_{cal} at 1200°C, and T_{sin} at 1300°C to obtain higher $(BH)_{max}$ through this route.

For increasing the reactivity, a few oxide additives are also examined by many researchers to enhance the diffusion of the reaction center. The accumulation of sintering aids has confirmed acceptable grain-growth regulation, yielding a dense body with good magnetic properties. In this regard, (Sözeri et al., 2012) have doped B_2O_3 (1 wt%) as a crystal growth inhibitor for the formation of single-phase SrM at low temperatures (below 1050°C). (Kostishyn et al., 2015, 2016) have also reported the doping of B_2O_3 (<1.5 wt%) in the solid-state route of SrM, which shows an increase in H_c with a decrease in M_r. (Töpfer et al., 2005) have reported improved magnetic properties of SrM with the doping of 0.5 wt% SiO_2 and 0.5 wt% $CaCO_3$ as sintering aids. (Qiao et al., 2010) have observed an improvement in the magnetic properties through morphological modification with the doping of Bi_2O_3. This processing technique generally synthesizes the material with the particle size of a nanometer to micrometer order. Significant reduction in crystallite size (107 nm to 40 nm) may also be attained through high-energy ball milling with PVA (25%) and $SrFe_{12}O_{19}$ (75%), as reported by *Gonzalez et al*. (Tenorio Gonzalez et al., 2019).

1.5.2 Hydrothermal Process

It is a synthesis process in which the solution of precursors and an appropriate base, generally water, is autoclaved. A temperature of 100-374°C (i.e., in the middle of the boiling and critical point of the solvent) and a maximum pressure of 22.1 MPa (vapor pressure of solvent at its critical point) are applied for the reactant reactions to get the desired product (Rahaman, 2017). Then the outcome is washed with a dilute mixture of HCl/deionized water/alcohol to remove the unreacted precursors. After that, the product is dried and calcined (if required) at a relatively low calcination temperature than the traditional process.

This process is optimized for SrM by many researchers. In this process, (Jean et al., 2010; Xia et al., 2013; Zhang et al., 2016) have optimized the Fe^{3+}/Sr^{2+} molar ratio (R_M) to 8:1 for better purity and phase formation of SrM. (Zhang et al., 2016) have also conveyed that better magnetic properties of SrM can be achieved with R_M of 8. (Hilczer et al., 2014) have found that the annealing process can favor the magnetic and dielectric properties of hydrothermally synthesized SrM. (Xia et al., 2013) have reported that an increase in sintering temperature (1200°C) can result in better M_s and H_c values, and it should be either equal to or more than 1050°C (Dang et al., 2012). In this process, the desired phases are generally obtained during the synthesis procedure, which rectifies the need for calcination. It can produce a narrow particle-size distribution with moderate purity and chemical homogeneity.

1.5.3 Co-precipitation Process

This method is used for getting high-purity, homogeneous particles. In this technique, precursors are taken into a stoichiometric ratio and dissolved into the distilled water at 90°C. Then, sodium hydroxides are gradually added to maintain the solution at ~10 pH with continuous stirring. After the complete dissociation of the precipitated material, it is filtered and washed with deionizing water. Then the material is kept at 80-100°C for drying. Finally, the dried material is calcined to get the desired phase at a suitable temperature.

(Drmota et al., 2010) have optimized the T_{cal} at 800°C and R_M at 6.4 for a high value of M_s through this process. They have reported a gradual decrease in M_s with an increase in both T_{cal} and R_M. (Ganjali et al., 2013) have studied the effect of T_{cal} and reported a M_s of 60.53 emu/g and H_c of 5 kOe at 1000°C. (Tan & Chen, 2013) have found reasonable ferromagnetism at T_{sin} of 1000°C. A novel approach in the co-precipitation process of SrM is carried out by (Rashad & Ibrahim, 2011) with better magnetic properties, like M_s of 85.4

emu/g and H_c of 4.9 kOe at 1000^{o}C annealing temperature. (Hessien et al., 2008) have reported the irregular shape and size of SrM particles and the consistency of some intermediate non-ferromagnetic phases through this method. Usually, this process is used to synthesize the metal oxides, but it is an avoidable process for enhancing the magnetic properties of SrM.

1.5.4 Sol-gel Process

The process is well-known for its controlled shape and narrowly distributed particle size. For high-sensitivity applications, these types of magnetic particles are necessary. It results in the material with high magnetic properties being obtained at a relatively low calcination temperature (Sapoletova et al., 2015). The fine particles of the compound are suspended in a liquid (termed as sol). Suspended particles are then changed into a highly viscous mass (gel) with a stable heating temperature. The starting materials are generally metal alkoxide with suitable alcohol. The stoichiometric amounts of precursors are dissolved in the distilled water and kept at 50-90^{o}C temperature with continuous stirring. The solution is dried conventionally until a very high mass gel is formed through evaporation. This gel is then crushed, ground, and subsequently calcined to get pure phases.

In this process, (García-Cerda, 2004) have conveyed to keep a low T_{cal} (800^{o}C or < 900^{o}C) to avoid the formation of transitional phases and have reported good magnetic properties in SrM. Increasing T_{cal} > 900^{o}C would result in larger particle size; hence, a huge reduction in H_c with an increase in M_s can be observed (Teh et al., 2011). (Nga et al., 2014) have studied the effect of Fe/Sr ratio (R_M), pH, calcination temperature, and time in the sol-gel synthesis of SrM. The formation of single-phase SrM is optimized at T_{cal} of 850^{o}C with ~1 pH and 10.5 R_M. (Wang et al., 2009) have also reported the same $T_{cal,}$ about 850^{o}C but R_M at 11.5. High purity with better powder homogeneity can be acquired through this process, but the metal alkoxides are expensive, which can increase the processing cost.

1.5.5 Sol-gel Auto-combustion method

The auto-combustion method is a versatile and self-propagating synthesis technique. It is widely used in the synthesis of SrM. This process is similar to the sol-gel except for the fuels, which are added in this method with precursors. After the gel formation, the temperature is raised to 200-250^{o}C, which causes the self-propagating combustion of viscose gel and results in a high volumetric powder. The outcome is further calcined to get the desired product.

(Doroftei et al., 2006) have identified that the resulting powders obtained through this method demonstrate low H_c with relatively high M_s. T_{ann} ~1000^{o}C is reported as the most suitable temperature to optimize both M_s and H_c. They have conveyed that increasing T_{ann} with a reduction in time or vice-versa could result in a rich improvement of H_c. (Zhanyong et al., 2010) have adopted a microwave-assisted calcination process, which results in the ultrafine SrM particle in less temperature and time. For a high $(BH)_{max}$ value, the calcination time of 120 min is found to be more effective by them. The main advantage of auto-combustion is the ultrafine powder particles that have excellent homogeneity and narrow particle size distribution. The dependency of magnetic properties on particle size makes it the most favorable synthesis process.

A summarized Table 1.3 is given to visualize the effect of various synthesis routes and different synthesis parameters along with the variation in magnetic properties of pristine strontium hexaferrite. For achieving high H_c values in a material, single-domain particle size may be helpful. In this contrast, sol-gel auto-combustion is a well famous and versatile synthesis process that can result in a very small, homogeneous, and narrowband distribution of particles at a relatively cheap and fast rate (Eikeland et al., 2018). Also, extrinsic magnetic properties like M_r and H_c are susceptible to particle shape and size, which could be better controlled by the sol-gel auto-combustion process.

Table 1.3 *Comparison of various synthesis routes of SrM with magnetic properties.*

Synthesis process	Fe/Sr ratio	Heat treatment	Properties @300K	Reference
Solid-state	12	T_{cal}=1100°C/4h, T_{sin}=1250°C/2h	M_s = 71.8 emu/g, H_c = 4.12 kOe	(Lim et al., 2018)
Solid-state	12	T_{cal}=1100°C/1h	M_s = 66.9 emu/g, H_c = 3.3 kOe	(Koohdar et al., 2009)
Hydrothermal	8	T_{ann}=1000°C/3.3h	M_s = 76 emu/g, H_c = 1.88 kOe	(Jean et al., 2010)
Hydrothermal	11	T_{cal}=1050°C	M_s = 66 emu/g, H_c = 6.32 kOe	(Dang et al., 2012)
Co-precipitation	9.23	T_{ann}=1000°C/2h	M_s = 84.15 emu/g, H_c = 4.43 kOe	(Hessien et al., 2008)
Co-precipitation	8.57	T_{ann}=1000°C/2h	M_s = 74.12 emu/g, H_c = 3.46 kOe	(Hessien et al., 2009)
Sol-gel	12	T_{cal}=1000°C	M_s = 85 emu/g, H_c = 4.5 kOe	(Wong et al., 2014)
Sol-gel	12	T_{ann}=900°C/2h	M_s = 71.3 emu/g, H_c = 4.9 kOe	(Das et al., 2015)
Auto-combustion	12	T_{cal}=1000°C	M_s = 73.54 emu/g, H_c = 5 kOe	(Abraime et al., 2017)
Auto-combustion	12	T_{ann}=1000°C/5h	M_s = 74.26 emu/g, H_c = 5.67 kOe	(Roohani et al., 2015)

1.6 Literature Survey on Substitutional Efficacy of Non-REEs in SrM

Combining different magnetic materials is the way to develop a stronger magnet than the existing ones. In SrM, the optimized substitution of elements at the Sr or Fe site is more decisive for upgraded magnetic properties. The spin orientations of Fe ions are coupled through O^{2-} ions by superexchange interaction according to the antiferromagnetic theory of the Néel model (Park, 2016) and play a dynamic role in magnetic characteristics.

The effect of various substituted elements (non-REEs) in SrM structure is best tried to cover, which may help to select appropriate substituting elements in SrM to formulate it as a well-suited permanent magnet.

Cobalt (Co^{2+}) ions generally replace Fe ions at $4f_2$ (↓), $2b$ (↑), and $2a$ (↑) lattice sites (Liu et al., 2012). In SrM structure, it causes the utmost influence in K. In study of a composition $SrFe_{12-x}Co_xO_{19}$ ($0 \leq x \leq 1$) by (Roohani et al., 2017), a maximum value of M_s = 78.89 emu/g with H_c of 1.33 kOe is obtained at x = 0.5. They have found an increase in M_s till x = 0.5, which reduces with further substitution, whereas a rapid drop in H_c is observed with Co content. The reduction of M_s is explained by the replacement of Fe ions from spin-down sites $4f_1$ (↓) and $4f_2$ (↓). It causes an increase in net magnetic moment due to Co ($3\mu_B$) substitution at Fe ($5\mu_B$) sites, thereby resulting in the improvement of M_s. High Co ions (x > 0.5) have tendency to occupy $12k$ (↑) site, which decreases several up-spin and causes M_s reduction. A decrease in K indorses the decrease in H_c due to $4f_2$ (↓) and $2b$ (↑) sites. In a study by (Liu et al., 2012) for $0 \leq x \leq 0.2$, an increase in M_s is reported at x = 0.2 with a decrease in H_c than the pure SrM. M_s does not change significantly for low Co concentration (x < 0.2). In the same composition for $0 \leq x \leq 0.3$, an initial decrease in M_s is observed by (Xie et al., 2012) with Co content ($x \leq 0.1$), which starts increasing for $x \geq 0.15$. $4f_2$ (↓) and $2a$ (↑) site occupancy is explained for such kind of substitutional behavior. (Wu et al., 2017) have reported a decrease in M_s by Co ion substitution due to lattice strain. They have obtained M_s of 91.3emu/g at T_{cal} of 950°C, which is found in detrimental mode with an increase in T_{cal} and Co content. Substitution of Co ion at Sr site may also be favorable for M_s improvement as it increases the net magnetic moment in the DFT study by (Lamouri et al., 2021). In a study of $SrAl_4Fe_{8-x}Co_xO_{19}$ ($0 \leq x \leq 1$) by (Shekhawat & Roy, 2019), Co substitution is found to enhance the M_s and M_r values but at the expense of H_c. They have explained Co as a densification prompting element and responsible for grain

growth in the samples. Increased grain size is one of the reasons for a consistent decrease in H_c with Co substitution. Enhancement in M_s is explained by the occupying tendency of Co ions at $4f_1$ and $4f_2$ sites. The low magnetic moment of Co ions reduces the net up-spin moment and results in an increment of M_s value. Density enhancement of compositions is also a reason for improved M_s due to an increase in spin rotation. Overall Co^{2+} substitution can be a suitable choice for the M_s improvement of SrM magnets.

Zinc (Zn^{2+}) ions mainly occupy the $4f_1$ (↓) site of Fe^{3+} ions, which results in the enhancement of M_s value (Haq & Anis-ur-Rehman, 2021). However, high content ($x \geq 0.2$) of Zn^{2+} ion may occupy *12k*, *2a*, and/or *2b* lattice sites causing the reduction in M_s (Nguyen et al., 2021). If Zn ions occupy the *2b* site, it will cause a reduction in both M_s and H_c parameters (Banihashemi et al., 2021). Substitution of Zn ion in BaM is reported to incline the magnetic properties of BaM towards a soft magnet (Nuraini et al., 2015). A similar dilution in H_c may also be observed in SrM, with an increase in M_s value for a small amount of Zn substitution (Tiwari et al., 2016). The effect of Zn-Mn substitution in $SrFe_{12-2x}Zn_xMn_xO_{19}$ ($0 \leq x \leq 0.4$) is trialed by (Kang et al., 2015). For $x \leq 0.2$, M_s is slightly higher than pure SrM. Yet, M_s and H_c uninterruptedly decrease with Zn-Mn content. Zn and Mn ion prefer $4f_1$ (↓) or $4f_2$ (↓) sites implying an increase in M_s, which decreases for higher substitutional amounts due to a decrease in net magnetic moment. The effect of Zn-Mn in $SrFe_{12-2x}Zn_xMn_xO_{19}$ ($0 \leq x \leq 1$) has been studied by (Arab et al., 2015). Improvement in M_s and H_c is found with T_{ann}. Both M_s and H_c have shown approximately a similar trend and have reached the maximum at x = 0.6. They have explained the trend of M_s by a decrease in superexchange interaction and the occupancy of Zn ions at $4f_1$ (↓) site for $x < 0.6$, and at *2a* (↑) site for $x > 0.6$, and. Zn-Zr substitution in $SrFe_{12-2(x+y)}Zn_xZr_yO_{19}$ ($0.5 \leq x, y \leq 2$) have studied by (Abdellahi et al., 2018), where a remarkable increase in M_s (108 emu/g) is obtained at x, y = 1. M_s initially increases till x, y = 1, then decreases with the further

substitutional amount. The substitution of Zn-Zr decreases the H_c values bizarrely compared to pristine SrM. Zn-Zr substitution replaces Fe ions at $4f_1$ (↓) and $4f_2$ (↓) sites and improves M_s value. A sudden decrease in M_s for high substitutional content is caused due to the weakening of superexchange interaction. A decrease in K may justify H_c behavior due to $4f_1$ (↓) and $2b$ (↑) sites. Zn-Zr substitution is also studied by (Iqbal et al., 2009) with the effect of T_{ann} in $SrFe_{12-2x}Zn_xZr_xO_{19}$ ($0 \leq x \leq 0.8$). For 1120°C of T_{ann}, M_s steadily increase with a decrease in H_c due to the particle size effect. They have conveyed an increase in both M_s and M_r till $x \leq 0.4$. In $SrFe_{12-2x}Zn_xCr_xO_{19}$ ($0 \leq x \leq 0.8$), a drop is observed for both H_c and M_s with the substitutional amount (Asghar & Anis-Ur-Rehman, 2012). $SrFe_{12-x}(Zn_{0.7}Nb_{0.3})_xO_{19}$ for ($0 \leq x \leq 1$) is analyzed by (Fang et al., 2004). They have found an improvement in M_s and T_c with a decrease in H_c due to substitution. It signifies that the substitution of Zn^{2+} ions can be considered for M_s improvement.

Nickel (Ni^{2+}) substitution for $SrFe_{12-x}Ni_xO_{19}$ (x = 0-1) composition is studied by (Roohani et al., 2018). They have observed a continuous increase in M_s till $x \leq 0.75$, which decreases slightly with further Ni content. In contrast, H_c is observed to reduce continuously with the substitutional amount. For low content $x \leq 0.75$, Ni ions preferentially occupy $4f_1$ (↓) and $4f_2$ (↓) sites. Ni^{2+} ($2\mu_B$) ion substitution at Fe^{3+} ($5\mu_B$) sites results in a reduction of spin-down moment and hence, improvement in the net magnetic moment and subsequent improvement in the M_s value. For $x \geq 0.75$, Fe ions are replaced from $12k$ (↑) site, which causes a decrease in up-spin moment, and so a reduction in M_s is observed. H_c declination is validated by a decrease in K due to $4f_2$ (↓) and $2b$ (↑) site occupancy of Ni ions and smaller grain size of particles. (Mousavi Ghahfarokhi et al., 2015) have reported that a very small amount of Ni^{2+} substitution (x=0.01) in the SrM structure would result in an initial increase of M_s value followed by a decrease till x = 0.2 in $SrFe_{12-x}Ni_xO_{19}$ (x = 0-1). After x > 0.2, M_s again shows an escalation. Meanwhile, H_c decreases with substitution content.

The maximum value of M_s is obtained at 61.62 emu/g with H_c of 3.56 kOe at x = 0.01. They have conveyed that for low substitution x < 0.2, Ni ions possess a preference to occupy the $4f_2$ (↓) site, whereas they may occupy *12k* (↑) and *2a* (↑) sites for further Ni substitution. Substitution of Ni ions also affects the easy direction of magnetization, thereby resulting in a decrease in *K*. Reduction in *K* leads to a diminishing H_c value. The lattice site occupancy of Ni ion results in the observed M_s behavior.

Aluminum (Al^{3+}) substitution at the Fe site is found to be the most suitable element for increasing the H_c value of strontium hexaferrite magnet. The effect of Al^{3+} ($0 \leq x \leq 12$) substitution in $SrFe_{12-x}Al_xO_{19}$ is studied by (Luo et al., 2012), and a significant value of H_c = 18.1 kOe is reported for $SrFe_8Al_4O_{19}$ but with a very small M_s of 9 emu/g. The values of M_s, M_r, and T_c are found in a decreasing trend till x < 6. A small amount of substitution ($x \leq 1$) declines the H_c value than pristine SrM and starts increasing with further substitution and attains the maximum at x = 4, followed by a drastic decrease for $x \geq 6$, as shown in Fig 1.5. After x > 6, samples gradually tend to paramagnetic behavior. In SrM, *2a*, *2b*, and *12k* lattice sites mainly contribute to the magnetic properties. Al^{3+} ions possess an occupying tendency towards *12k* (↑), *2a* (↑), and $4f_1$ (↓) lattice sites (Chen et al., 2008). A decrease in M_s and M_r has resulted from the substitution of Al^{3+} at *12k* (octahedral) site of Fe ion and reduction in superexchange interaction between Fe_A^{3+}-O^{2-}-Fe_B^{2+}. The *2b* (↑) lattice site plays a decisive role in determining *K* and hence H_c. A low concentration of Al^{3+} ion does not occupy *2b* (↑) site; hence it may result in a declining behavior of H_c for $x \leq 1$. For a higher substitutional amount of Al^{3+} ($x \geq 4$), some Fe^{3+} ions are replaced by Al^{3+} from the *2b* site, resulting in improved H_c. (Wang et al., 2017) have also reported the same behavior of M_s in $SrFe_{12-x}Al_xO_{19}$ for $0 \leq x \leq 4$. They have found an increase in H_c with Al content, and the maximum H_c of 16.88 kOe is obtained at x = 3. However, for x = 4, it is reduced

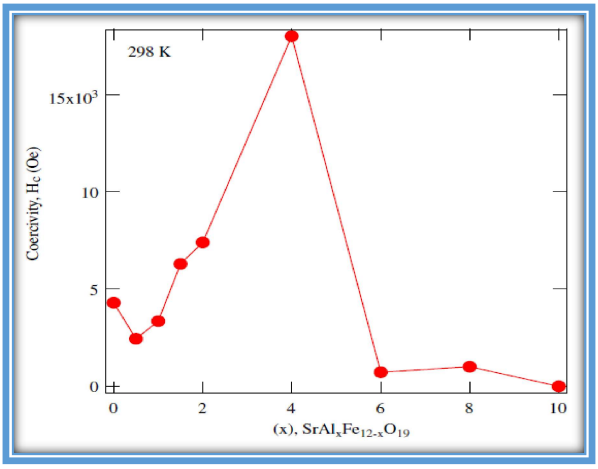

Figure 1.5 *Variation in H_c parameter with Al-substitution in $SrFe_{12-x}Al_xO_{19}$. Reprinted with permission from* (Luo et al., 2012).

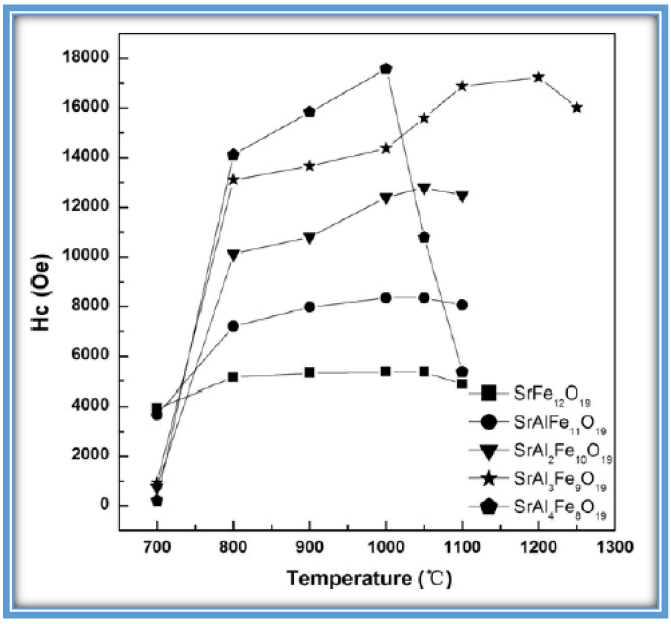

Figure 1.6 *Variation pattern of H_c with Al substitution and annealing temperature (T_{ann}) in SrM. Reprinted with permission from* (Wang et al., 2012).

drastically. This reduction is explained by a decrease in net magnetic moment close to zero and weak exchange interaction between Fe ions. In another study by (Wang et al., 2012), the highest H_c = 17.57 kOe is obtained for $SrFe_8Al_4O_{19}$ at T_{ann} of 1000°C, which is reduced with the further increase in T_{ann}. In this study, the effect of Al substitution is studied in $SrFe_{12-x}Al_xO_{19}$ ($0 \leq x \leq 4$) simultaneously with T_{ann}, and the varying pattern of H_c with different T_{ann} and Al^{3+} substitution amounts are shown in Fig. 1.6. In pure SrM, the value

of M_s increases with T_{ann}; however, it is not valid for Al-substituted SrM. In the annealing temperature range of $800^oC \leq T_{ann} \leq 1000^oC$, H_c is in positive drift with the substitutional amount of Al ion. In the study of (Torkian et al., 2016), a decrease in M_s, T_c, and magnetocrystalline anisotropy is observed in $SrFe_{12-x}Al_xO_{19}$ ($0 \leq x \leq 4$) due to the substitution of Al ion. Several researchers also explore Al substitution, and approximately similar variations in magnetic characteristics are revealed. It is the most promising substitution element in SrM magnet regarding H_c enhancement but at the expense of M_s.

Chromium (Cr^{3+}) ions have an occupying tendency to *2a* (↑), *12k* (↑), and *4f1* (↓) lattice sites of Fe ions (Katlakunta et al., 2015). In the study of $SrFe_{12-x}Cr_xO_{19}$ for $0 \leq x \leq 1$, (Slimani et al., 2018) have observed an increment in M_s, Mr, and H_c values for $x \leq 0.4$, which are reduced with further substitution. Maximum M_s is observed at x = 0.2, while H_c attains its maximum at x = 0.4. The reason for the M_s reduction is due to the lower magnetic moment of Cr^{3+} ($3\mu_B$) ion than the Fe^{3+} ($3\mu_B$) ion, which replaces Fe in up-spin direction. In $SrFe_{12-x}Cr_xO_{19}$ ($0.1 \leq x \leq 0.9$), a consistent decrease in M_s and M_r values but an increase in H_c with Cr^{3+} content is observed by (Katlakunta et al., 2015). The highest H_c of 7.335kOe with M_s of 30emu/g is attained at x = 0.9. They have described the lower magnetic moment of Cr ion as the reason for M_s reduction, which replaces Fe ion from *2a* (↑) or *12k* (↑) lattice site, and the smaller size of grains is responsible for H_c increment. (Praveena et al., 2015) have also observed a similar effect of Cr^{3+} ion substitution in $SrFe_{12-x}Cr_xO_{19}$ ($0 \leq x \leq 0.9$). (Nourbakhsh et al., 2011) have found that x = 0.3 can cause an increase in M_r and a decrease in H_c values of $SrFe_{12-x}Cr_xO_{19}$ ($0 \leq x \leq 0.5$). Enhanced grain growth may be the reason for this behavior. (Fang et al., 2005) have observed an increase in M_s for low substitutional content ($x \leq 0.4$), which reduces with a higher amount of substitution in $SrFe_{12-x}Cr_xO_{19}$ ($0 \leq x \leq 1$). They have found that H_c reduces for $x \leq 0.5$ and then increases for $x \geq 0.6$. The reason for M_s increment is given by more occupied sites of Cr ions in *4f2* (↓) than *2a* (↑) and

12k (↑), whereas α-Fe_2O_3 phases cause a reduction in M_s. The decrease in H_c is attributed to *K* reduction and decrease in *c/a* ratio. However, H_c increment for $x \geq 0.6$ may be caused by the resistive grain boundaries. (Huang et al., 2015) have examined the effect of T_{sin} with Cr concentration in $SrFe_{12-x}Cr_xO_{19}$ ($0 \leq x \leq 0.6$). They have reported an increase in M_s and M_r with a decrease in H_c value due to high sintering temperatures. They have obtained a positive trend of H_c with declination in M_s due to increased Cr^{3+} ion content. They have observed a noticeable increase in $(BH)_{max}$ because of additives ($CaCO_3$, SiO_2); meanwhile, a slight addition in $(BH)_{max}$ is observed with an increase in T_{sin}. (Zahid et al., 2022) have examined the substitutional behavior of Cr^{3+} ion at Sr site for $Sr_{1-x}Cr_xFe_{12}O_{19}$ ($0 \leq x \leq 0.5$). They have proposed that substituting Cr^{3+} ion at Sr lattice site may improve the M_s and H_c values. It will cause some Fe^{3+} ions at *4f₂* (↓) to change in Fe^{2+} for maintaining the charge neutrality, which reduces the concentration of Fe^{3+} at *4f₂* and improves the net magnetic moment; hence increase in M_s. The smaller ionic radius of Cr ion than Sr ion may improve the magnetocrystalline anisotropy, which might help in achieving high H_c value. Substitution of an optimal amount of Cr^{3+} ion at Fe and Sr site can be considered for increasing the H_c value of SrM with a sufficient value of M_s as well.

Manganese (Mn^{3+}) ions have the propensity to replace Fe ions from all five lattice sites. In the study of $SrFe_{12-x}Mn_xO_{19}$ ($0 \leq x \leq 5$) by (Tenorio-González et al., 2017), a consistent trend of M_s and M_r is experienced with Mn^{3+} substitution. H_c increases remarkably with Mn and reaches a maximum value of 9.7 kOe at x = 5 with M_s of 34.8 emu/g. The decrease of M_s is given by occupancy of Mn^{3+} ions at *2a* (↑) and *12k* (↑) sites, while H_c increment is justified by increased microstrain. (Silva et al., 2015) have reported the substitutional effect of low Mn^{3+} content as $SrFe_{11.9}Mn_{0.1}O_{19}$. In their result, the values of all M_s, M_r, and H_c are reduced compared to pristine SrM, and samples are inclined towards soft magnet characteristics. Substitution of Mn^{3+} ions may result in strong

magnetic dipole coupling, which may cause a decrease in H_c. M_s reduction is associated with Mn^{3+} preference to *2a* (↑) and *12k* (↑) lattice sites, which reduces the net magnetic moment due to lesser magnetic moment of Mn^{3+} ($3.5\mu_B$) ion than Fe^{3+} ($5\mu_B$) ion. Spin canting could also be a reason for such reduction in M_s value. Mn^{2+} ions have a magnetic moment of $5\mu_B$, which is equal to the Fe^{3+} ion. So, Mn^{2+} substitution does not affect the net magnetic moment. Due to Mn^{2+} substitution, if Fe^{3+} ($5\mu_B$) are transformed in Fe^{2+} ($4\mu_B$), M_s will eventually improve. In that case, Mn^{2+} ($5\mu_B$) may convert into Mn^{3+} ($3.5\mu_B$) to balance the charge neutrality of SrM and hence, contribute to the M_s up-gradation.

Copper (Cu^{3+}) substitution prefers to occupy the octahedral lattice site of Fe^{3+} ion (Anantharamaiah et al., 2020). Cu^{3+} ($1\mu_B$) ions can enhance the M_s value by increasing the net magnetic moment and intensifying the superexchange interaction between Fe^{3+} ions (Maramu et al., 2021). Substitution of Cu ion at Fe site does not change the hard magnetic characteristics of SrM. However, Cu^{3+} incorporation at the Sr^{2+} site may result in a soft magnetic characteristic of SrM with a drastic decrease in M_s (Ajeesha et al., 2020).

Indium (In^{3+}) is a diamagnetic ion that has the occupying tendency to *4f₂* (↓) and *12k* (↑) lattice site of Fe^{3+} ion (Turchenko et al., 2022). With the increasing content of In^{3+} ($0\mu_B$) ion, exceeding multiplicity of *12k* site than the *4f₂* site causes a decrease in M_s value. Overall, the substitution of In^{3+} ion is reported to decrease both the M_s and H_c values due to a decrease in the net magnetic moment and reduced magnetocrystalline anisotropy (Turchenko et al., 2020, 2021, 2022; Zhou et al., 2021).

Ruthenium (Ru^{4+}) ion mainly occupies *2a* and *4f₁* lattice sites, with some at *4f₂* and *12k* lattice sites of Fe^{3+} ion in SrM. In a study of $SrFe_{12-x}Ru_xO_{19}$ ($0 \leq x \leq 1.5$) by (Chang et al., 2020), Ru^{4+} substitution severely reduces the H_c of material with a minute increase in M_s. (Sai et al., 2022) have explored the substitutional behavior of Ru-Zn ions in a composition of $SrFe_{12-2x}Zn_xRu_xO_{19}$ ($0.1 \leq x \leq 0.7$) and experienced lows H_c value along

with low M_s due to the substitution. In a study of $SrFe_{12-2x}Ni_xRu_xO_{19}$ ($x \leq 0.7$) by (Chang et al., 2020), incorporation of Ru ion in SrM structure is reported to enhance the M_s value, but a drastic drop in the H_c value is observed which change its magnetic behavior similar to a soft magnet.

Titanium (Ti^{4+}) substitution without other elements is not found in SrM. Yet, it is analyzed with other elements like Co and Zn. In a study of $SrFe_{12-2x}(CoTi)_xO_{19}$ ($0.5 \leq x \leq 3$) by (Zhang et al., 2019), Co-Ti substitution is observed to decrease the value of M_s continuously with the substitutional amount while it dilutes H_c very much than SrM. The same composition for $0 \leq x \leq 1.25$ is also studied by (Liu et al., 2019b). With the substitution, they have attained a maximum M_s of 83.8 emu/g with H_c of 1.013 kOe. In both Co-Ti substitution studies, the soft magnetic characteristic of samples is revealed, which is also confirmed by (Vinaykumar & Bera, 2019). Ti-Zn substitutional effect in $SrFe_{12-2x}Ti_xZn_xO_{19}$ ($0 \leq x \leq 1$) with T_{ann} is analyzed by (Fang et al., 2001). Both M_s and H_c are observed to increase up to 950°C of annealing temperature while both decrease with Ti-Zn content. A similar effect of Ti-Zn substitution is also observed by (Baniasadi et al., 2014) in $SrFe_{12-x}Ti_{x/2}Zn_{x/2}O_{19}$ ($0 \leq x \leq 2.5$). They have explained that a reduction in H_c has resulted from a decrease in K and M_s deterioration is related to the substitutional preference of Ti-Zn ions at *2a* (↑), *2b* (↑), and *12k* (↑) lattice sites. These site occupancies cause a decrease in net magnetic moment and weakening of superexchange interaction between Fe ions, hence a decline in M_s value.

Tin (Sn^{4+}) ions have a preference to occupy *12k* (↑) and *4f₂* (↓) sites where the probability at *12k* is higher (Dixit et al., 2019). Substitutional behavior of Sn^{4+} in a $SrFe_{12-4x}Sn_{2x}Co_xZn_xO_{19}$ ($0 \leq x \leq 0.7$) composition is explored by (Ghezelbash et al., 2018). In their study, a random behavior of M_s is obtained with the substitution while H_c decreases drastically till $x \leq 0.5$, followed by a slight increase at $x = 0.7$. The formation of α-Fe_2O_3

phases is responsible for such variation in M_s. A composition of $SrFe_{12-x}(Sn_{0.5}Mg_{0.5})_xO_{19}$ ($0 \leq x \leq 1$) has been studied by (Davoodi & Hashemi, 2011). They have reported a consistent increase in M_s with deterioration in H_c. These magnetic properties may result from the occupancy of Sn^{4+} and Mg^{2+} ions at the $4f_2$ (↓) site.

Table 1.4 *Compiled substitutional effect of various non-rare-earth elements in magnetic properties of SrM with M_s and H_c values.*

Element	Composition	Magnetic Properties @300K	Reference
Al	$SrFe_8Al_4O_{19}$	M_s = 32.2 emu/g, H_c = 8.45 kOe	(Torkian et al., 2016)
Al	$SrFe_8Al_4O_{19}$	M_s = 12.25 emu/g, H_c =18.85 kOe	(Shekhawat & Roy, 2019)
Al, Ca	$Sr_{1-4/12}Ca_{4/12}Fe_8Al_4O_{19}$	M_s = 12.7 emu/g, H_c = 21.3 kOe	(Trusov et al., 2018)
Cr	$SrFe_{11.1}Cr_{0.9}O_{19}$	M_s = 30 emu/g, H_c = 7.3 kOe	(Katlakunta et al., 2015)
Cr	$Sr_{0.7}Cr_{0.3}Fe_{12}O_{19}$	M_s = 57 emu/g, H_c = 6.24 kOe	(Zahid et al., 2022)
Mn	$SrFe_7Mn_5O_{19}$	M_s = 34.8 emu/g, H_c = 9.7 kOe	(Tenorio-González et al., 2017)
Mn, Zn	$SrFe_{11.8}Mn_{0.1}Zn_{0.1}O_{19}$	M_s = 74.4 emu/g, H_c = 3.62 kOe	(Kang et al., 2015)
Cu	$SrFe_{11.2}Cu_{0.8}O_{19}$	M_s = 72 emu/g, H_c = 6.68 kOe	(Maramu et al., 2021)
In	$SrFe_{11.9}In_{0.1}O_{19}$	M_s = 85 emu/g, H_c = 4.19 kOe	(Turchenko et al., 2020)
Ni	$SrFe_{11.8}Ni_{0.2}O_{19}$	M_s = 61.62 emu/g, H_c = 3.56 kOe	(Mousavi Ghahfarokhi et al., 2015)
Co	$SrFe_{11.25}Co_{0.75}O_{19}$	M_s = 78.48 emu/g, H_c = 1.29 kOe	(Roohani et al., 2017)
Co, Ti	$SrFe_{10.5}Co_{0.75}Ti_{0.75}O_{19}$	M_s = 83.8 emu/g,	(Liu et al., 2019b)

		H_c = 1.013 kOe	
Zn, Ti	$SrFe_{11.6}Zn_{0.2}Ti_{0.2}O_{19}$	M_s = 70 emu/g, H_c = 6.2 kOe	(Fang et al., 2001)
Zn, Zr	$SrFe_{10}ZnZrO_{19}$	M_s = 108 emu/g, H_c = 27 Oe	(Abdellahi et al., 2018)
Zn, Zr	$SrFe_{11.7}Zn_{0.15}Zr_{0.15}O_{19}$	M_s = 82.16 emu/g, H_c = 6.09 kOe	(Kumar Godara et al., 2022)
Zn, Nb	$SrFe_{11.2}(Zn_{0.7}Nb_{0.3})_{0.8}O_{19}$	M_s = 73 emu/g, H_c =3.1 kOe	(Q. Fang et al., 2004)
Zr	$Sr_{0.9}Zr_{0.1}Fe_{12}O_{19}$	M_s = 49.19 emu/g, H_c = 5.26 kOe	(Almessiere et al., 2019)
Zr, Cd	$SrFe_{11.6}Zr_{0.2}Cd_{0.2}O_{19}$	M_s = 90 emu/g, H_c = 1.26 kOe	(Ashiq et al., 2009)
Bi	$SrFe_{11.8}Bi_{0.2}O_{19}$	M_s = 53.2 emu/g, H_c = 3.57 kOe	(Auwal et al., 2016)
V	$SrFe_{11.98}V_{0.02}O_{19}$	M_s = 58.7 emu/g, H_c = 4.2 kOe	(Almessiere et al., 2019)
Pb	$SrFe_{11.6}Pb_{0.4}O_{19}$	M_s = 41.62 emu/g, H_c = 6.02 kOe	(Ramay et al., 2014)
Pb	$Sr_{0.95}Pb_{0.05}Fe_{12}O_{19}$	M_s = 46.65 emu/g, H_c = 2.84 kOe	(Ullah et al., 2013)
Ga	$SrFe_8Ga_4O_{19}$	M_s = 26.1 emu/g, H_c = 6.4 kOe	(Gorbachev et al., 2021)

The substitutional effect of different non-REEs on the magnetic properties of the strontium hexaferrite is compiled in Table 1.4. Some elements like Al, Cr, Mn are found to increase the H_c value of SrM significantly, while some elements like In, Co, Co-Ti, Zn-Zr, Zn-Ti, Zn-Mn, Zr-Cd, Cu are observed to increase the M_s value of SrM considerably. Improving both the magnetic parameters M_s and H_c is a great challenge that is required for the high $(BH)_{max}$ value. In this concern, an exchange-coupled magnet model given by (Kneller & Hawig, 1991) can be helpful. In this model, a high M_s soft magnetic material is

added to a high H_c hard magnetic material to enhance the M_r value through the exchange coupling of the hard magnetization phase with a soft magnetization phase by the interphase interface at the nanoscale level. Considering the idea of Kneller & Hawig model, the selection of substituted elements for the thesis work is based on their effect on the magnetic properties of SrM magnet, where one may improve M_s value while the other may improve H_c value.

1.7 Scope and Objective of the Present Work

In view of a cost-effective, eco-friendly, and efficient permanent magnet, scientific communities are terrifically searching for a rare-earth-free permanent magnet that can meet the performance of RE-based permanent magnets and have capabilities to fulfill the current market demand of PMs in different application areas. Strontium hexaferrite magnets represent the largest magnet group being used nowadays by volume. They are hard magnets with attractive properties like magnetic tunability, decent magnetism, high resistivity, good thermal stability, and negligible eddy current losses. However, it has a small $(BH)_{max}$ value, which is drawing attention to improving the magnetic properties of SrM magnets further. The $(BH)_{max}$ of magnets is sensitive to the M_s and H_c values, which indicates a requirement for enhancement in the M_s and H_c values of SrM magnets. The magnetic properties of this magnet can be improved with the different optimization in synthesizing parameters, the substitutional behavior of various non-RE elements, and the doping of various additives. Toward the main objective of developing a rare-earth-free permanent magnet, all these approaches have been considered comprehensively where improvement in the magnetic and dielectric properties of SrM is studied in the present work as follows:

- Examine the effect of Co and Cr ion substitution at the Fe lattice site of the strontium hexaferrite.

- Examine the effect of Cr and Zn ion substitution at the Sr and Fe lattice site, respectively, of the strontium hexaferrite.
- Examine the effect of Ni and Al ion substitution at the Fe lattice site of the strontium hexaferrite.
- Examine the effect of Bi_2O_3 doping and different sintering temperatures in the Al-substituted strontium hexaferrite.
- Examine the effect of Zn and Al ion substitution at the Fe lattice site of the strontium hexaferrite.